J Clin Monit Comput (2017) 31:783–791
DOI 10.1007/s10877-016-9908-7

ORIGINAL RESEARCH

Reliability of transpulmonary pressure–time curve profile to identify tidal recruitment/hyperinflation in experimental unilateral pleural effusion

P. Formenti[1,2] · M. Umbrello[2] · J. Graf[1,3] · A. B. Adams[1] · D. J. Dries[4] · J. J. Marini[1]

Received: 29 November 2015 / Accepted: 14 July 2016 / Published online: 20 July 2016

Abstract The stress index (SI) is a parameter that characterizes the shape of the airway pressure–time profile (P/t). It indicates the slope progression of the curve, reflecting both lung and chest wall properties. The presence of pleural effusion alters the mechanical properties of the respiratory system decreasing transpulmonary pressure (Ptp). We investigated whether the SI computed using Ptp tracing would provide reliable insight into tidal recruitment/overdistention during the tidal cycle in the presence of unilateral effusion. Unilateral pleural effusion was simulated in anesthetized, mechanically ventilated pigs. Respiratory system mechanics and thoracic computed tomography (CT) were studied to assess P/t curve shape and changes in global lung aeration. SI derived from airway pressure (Paw) was compared with that calculated by Ptp under the same conditions. These results were themselves compared with quantitative CT analysis as a gold standard for tidal recruitment/hyperinflation. Despite marked changes in tidal recruitment, mean values of SI computed either from Paw or Ptp were remarkably insensitive to variations of PEEP or condition. After the instillation of effusion, SI indicates a preponderant overdistension effect, not detected by CT. After the increment in PEEP level, the extent of CT-determined tidal recruitment suggest a huge recruitment effect of PEEP as reflected by lung compliance. Both SI in this case were unaffected. We showed that the ability of SI to predict tidal recruitment and overdistension was significantly reduced in a model of altered chest wall-lung relationship, even if the parameter was computed from the Ptp curve profile.

Keywords Stress index · Tidal recruitment · Tidal hyperinflation · Transpulmonary pressure · Pleural effusion · Respiratory mechanics

1 Introduction

Several mechanical ventilation strategies with the aim to avoid tidal hyperinflation and/or tidal recruitment have recently been proposed to prevent ventilator-associated lung injury. Parameters of respiratory mechanics, which are influenced by recruitment and derecruitment, have been investigated in theoretical models [1] and clinical studies [2]. It is usually assumed that the part of the respiratory system pressure–volume (P–V) curve above the upper inflection point (UIP) is the region where lung overdistension is prevalent, while the part below the lower inflection point (LIP) is the region of tidal recruitment prevalence [3]. Between these points, the "linear" portion of the curve is often considered to reflect a zone of safer alveolar expansion. It has been postulated that setting Positive End-expiratoy Pressure (PEEP) above LIP might

Electronic supplementary material The online version of this article (doi:10.1007/s10877-016-9908-7) contains supplementary material, which is available to authorized users.

✉ P. Formenti
formenti.paolo@fastwebnet.it

[1] Pulmonary Research Laboratory, Regions Hospital, St Paul, MN, USA

[2] Dipartimento di Anestesiologia e Terapia Intensiva, Azienda Opsedaliera San Paolo - Polo Universitario, Univeristà degli Studi di Milano, Via A. Di Rudinì, 8, 20142 Milan, Italy

[3] Departamento de Paciente Critico, Clinica Alemana de Santiago, Facultad de Medicina Clinica Alemana, Universidad del Desarrollo, Vitacura, Santiago, Chile

[4] Department of Surgical Services, HealthPartners Medical Group, University of Minnesota, Minneapolis/St. Paul, MN, USA

optimize alveolar recruitment [4]. Indeed, adjusting the inspiratory pressures above the LIP of the respiratory system P–V curve resulted in improved outcomes of patients with ARDS [5], even though ventilation pressures ranging between the LIP or UIP do not eliminate tidal recruitment or overdistension [6].

The stress index (SI) is a parameter that characterizes the shape of the airway pressure–time profile (P/*t*) during constant flow mechanical ventilation [7]. It is a "single compartment" concept that implies that the balance between recruitment and overdistension can be characterized by the curvature of the inflation P/*t* curve during constant flow and, therefore, of the P–V curve. SI is the exponent of an equation indicating the slope progression of the curve. A convex P/*t* curve indicates increasing compliance, representing preponderant tidal recruitment, whereas an upward concave shape in the P/*t* curve indicates decreasing compliance, representing preponderant tidal hyperinflation [8]. It has been well demonstrated how SI is of interest when the lungs are relatively uniform and surrounded by a normal chest wall. However, since both the lung and chest wall influence the SI [9], an alteration in chest wall characteristics, as that induced by a pleural effusion, can modify the mechanical properties of the respiratory system [10, 11], possibly affecting the discriminative ability of SI. Indeed, pleural effusion is accommodated by an expansion of chest wall volume and a contraction in lung gas volume [12]. In addition, by increasing the vertical gradient of pleural pressure (Ppl), pleural effusion decreases the transpulmonary pressure (Ptp)—the distending force of the lung [13, 14]. We have previously shown that in this specific setting of alterated chest wall-lung relationships, absolute values of SI are neither qualitatively nor quantitatively reliable as indicators of tidal recruitment or over-distention [15]. The use of esophageal pressure (Pes) to determine Ptp has drawn recent attention as a potential guide for lung-focused mechanical ventilation [16–18]. Some authors have suggested that Ptp curve should be used in place of Paw-based curve, as the former should only reflect lung characteristics, especially in presence of alterated chest wall properties [19].

Aim of the present experimental study was to investigate whether the SI computed using Ptp tracing would provide reliable insight into tidal recruitment/over distention during the tidal cycle in the presence of unilateral effusion.

2 Methods

An instillation of fluid into the pleural space replicated a unilateral pleural effusion in anesthetized, mechanically ventilated pigs. Respiratory system mechanics and thoracic computed tomography (CT) were studied to assess P/*t* curve shape and changes in global lung aeration.

2.1 Animal preparation

The protocol was approved by the Animal Care and Use Committee of Regions Hospital (St. Paul, MN). Five young healthy female Yorkshire pigs, mean weight 30.3 ± 2.5 kg were premedicated with intramuscular telazol/xylazine (2.2 and 6.6 mg/kg). After tracheotomy, 1 % isoflurane and 50 % oxygen in N_2O were delivered only for the remainder of the instrumentation period to perform femoral central venous and arterial catheter placement, suprapubic cystostomy and right pleurostomy.

A chest tube was inserted with a cephalad orientation at the level of the seventh intercostal space. Anesthesia was maintained thereafter only by continuous infusion of 20 mg/kg ketamine, 0.5 mg/kg acepromazine and 6.6 mg/kg mg xylazine in 500 mL normal saline starting at 20 mL/h, and titrated by physiologic assessment. Throughout the study animals remained paralyzed with hourly boluses of pancuronium 0.1 mg/kg and mechanically ventilated with an Engström Carestation^{TM} ventilator (GE Healthcare, Madison, WI): constant flow volume control ventilation, tidal volume (V_T) 9 mL/kg, respiratory rate titrated to an end-tidal CO_2 of 30–40 mmHg at baseline, inspiratory to expiratory ratio of 1:2 and FIO_2 of 0.5. Oxygen saturation, end-tidal CO_2, Paw, arterial pressure and heart rate were continuously monitored. An esophageal balloon catheter (SmartCath, CareFusion, San Diego, CA, USA) was placed to record Pes during ventilation. The balloon was airfilled with 2 mL, and at each step of the protocol the pressure reading was zeroed and the position was checked. Placement of the balloon in the stomach was confirmed by a transient increase in pressure during a gentle compression of the abdomen as previously described [15, 20]. The catheter was then slowly withdrawn into the esophagus, where pressure shows positive swings during inspiration. The catheter position posterior to the heart was confirmed by the positive occlusion test and by the appearance of cardiac pulsations on the waveform and by CT imaging (Online resource S1) [21, 22]. The direct measurement of pleural pressures in the normal pleural space is technically challenging because of the close approximation of the two pleural surfaces. Thus, a device introduced into a normal pleural space would lead to geometric distortion and result in deformation forces that are not representative of the pressure before the introduction of the device [23]. For these reasons, we decided to have an estimation of pleural pressure similar to the one used in clinical practice.

Respiratory system mechanics responses to pleural effusion and PEEP were studied. The animals also underwent sequential thoracic CT scan to assess changes in

global and regional lung aeration along with effusate distribution. At the end of each experiment, animals were euthanized by rapid injection of Euthasol®.

2.2 Experimental protocol

We compared values of SI derived from Paw with those calculated by Ptp under the same conditions (Fig. 1). These results were themselves compared with the extent of tidal recruitment and hyperinflation, as calculated using quantitative CT analysis. With the exception of PEEP, ventilator settings were unchanged throughout the experimental protocol. PEEP 1 and 10 cmH_2O were sequentially applied without recruitment maneuvers during baseline conditions (BSL) and after instillation of fluid into the right pleural space. We decided not to perform any recruitment maneuver between protocol steps because of the potential impact on the effects of PEEP in the study. We arbitrarily chose a "moderate" effusion volume of 16 mL/kg based on our previous experimental findings [24] in which we showed how this was enough to alter the chest wall-lung interaction. Thus, four consecutive steps were studied: baseline PEEP 1 (BSL P1), baseline PEEP 10 (BSL P10), pleural effusion PEEP 1 (PE P1), pleural effusion PEEP10 (PE P10). BSL measurements were taken after chest tube placement.

Airflow, Paw and Pes were measured through a D-lite+™ sensor (GE, Helsinki, Finland) placed between the Y-piece of the ventilator circuit and the endotracheal tube and connected to the airway module (E-COVX, GE, Madison, WI) of the ventilator (Online resource S1).

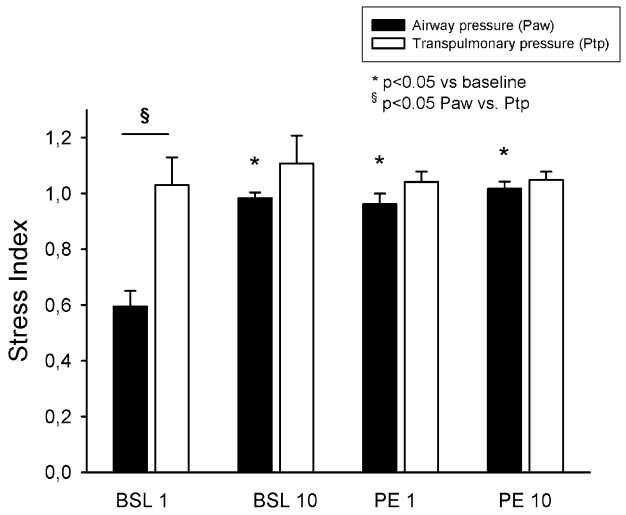

Fig. 1 The figure shows the values of Stress Index (SI) computed from airway pressure (Paw) and from transpulmonary pressure (Ptp) in each experimental conditions. Note the relatively narrow range of variation of the SI acrross varied conditions

Static compliance of the respiratory system (Crs) was calculated as

$$\mathrm{Crs} = \mathrm{Vt}/[\mathrm{Pplat} - (\mathrm{PEEP} + \mathrm{PEEPi})]$$

where Pplat represents plateau airway pressure after an inspiratory pause, and PEEPi corresponds to the elastic recoil pressure of the respiratory system at end-expiration that exceeds the externally set value. The use of the esophageal balloon catheter allowed us to partition Crs into its components of lung compliance (Cl) and Ccw with the following formulas:

$$\mathrm{Cl} = \mathrm{Vt}/\big[(\mathrm{Paw} - \mathrm{Pes})\ \text{end-inhalation} - (\mathrm{Paw} - \mathrm{Pes})\ \text{end-exhalation}\big]$$

and

$$\mathrm{Ccw} = \mathrm{Vt}/\big[(\mathrm{Pes} - \mathrm{Patm})\ \text{end-inhalation} - (\mathrm{Pes} - \mathrm{Patm})\ \text{end-exhalation}\big]$$

The constant inspiratory flow value was 20 L/min. Flow and pressure signals were exported from the ventilator through the RS-232 port, collected on a personal computer using a research data logging program for the ventilator (GE, Madison, WI) and stored as Excel™ files. Lung CT scans were acquired at each step at end-inspiration, by clamping the tracheal tube during an inspiratory occlusion, and at end-expiration. Helical CTs of the chest were obtained with a 64 slice CT scanner (LightSpeed™ VCT, GE Healthcare, Milwaukee, WI) using the following parameters: 120 kVp, 575 mA, collimation of 64 × 0.625 mm, pitch of 1, and gantry rotation time of 0.5 s. Images were reconstructed using the "STANDARD" kernel with a slice thickness of 2.5 mm and reconstruction field of view from 220 to 280 mm (pixel size from 0.43 to 0.55 mm).

2.3 CT analysis of lung aeration

End-expiration gas and tissue volumes of the lung were computed by compiling the frequency-distribution histograms of Hounsfield units from each slice of the CT scan. After an initial whole lung scan to determine the position of the diaphragm at end inspiration, the first eight supra-diaphragmatic slices were selected. During the CT, the eight selected slices were scanned at 0.4-s intervals. Lung dimensions were manually determined using Osiris CT analysis software [25, 26]. Tidal recruitment was calculated as the difference (Δ) in collapsed volume (−100–200 HU voxels) between end-expiration and end-inspiration, indexed to the corresponding Δ gas volume. Tidal hyperinflation was calculated as the Δ overinflated volume (−1000 to −900 HU voxels) at end-inspiration/end-expiration, indexed to the corresponding Δ gas volume.

2.4 Stress index analysis

Flow and pressure signals were examined for each single condition. The beginning and the end of each recorded breath were identified, as well as the longest portion of flow signal that fell within 3 % of the mean value of steady flow. Calculations were aborted if it was impossible to find out a constant flow signal because of artifacts, leakages or noise interference, and if the duration of the time interval was shorter than one-third of the inspiratory time, as recently suggested [27]. This only happened in <10 % of times. Once a single pressure-flow signal was obtained for each breath recorded (in total 28 ± 3), the stress index equation for both Paw and Pes ($P = a \times b + c$) was fitted to the pressure values of each breaths, using the Levenberg–Marquardt algorithm to achieve a "b" value (i.e. SI value) [5, 8] (Online resource F1). The calculations with an $R^2 < 0.95$ were excluded. In parallel, electronic subtraction of Paw–Pes generated a Ptp trace that was fitted to the SI equation to obtain the corresponding Ptp "b" values.

2.5 Statistical analysis

Based on preliminary experiments yielding an average baseline value of SI computed from Ptp of 1.0 ± 0.2, and considering that the amount of experimental pleural effusion we instilled is associated with a 30 % increase in tidal recruitment [24], we calculated that 4 animals were needed to detect a 30 % variation in the value of SI following pleural effusion, with a power of 80 % and $\alpha = 0.05$. For consistency with our previous work, we decided to enroll 5 animals.

Results are presented as mean ± SD if normally distributed, or median [1st; 3st quartile] if not; normality was assessed with Shapiro-Francia test. Given the repeated measure structure of the experimental design (each animal was subject to each experimental condition), comparisons among different steps were performed with repeated-measures analisys of variance if data were normally distributed; in case of pairwise multiple comparisons, the Holm-Sidak correction was applied. When normality test failed, RM-ANOVA on ranks was used, and the post hoc correction was performed with Tukey test. A Bland–Altman analysis of the comparison between SIpaw and SIptp in the different experimental conditions was computed (Online resource S3–S6). For all the comparisons, $p < 0.05$ was considered as statistically significant. Analysis was performed using Stata Statistical Software, release 11.0 (Stata Corporation, College Station, TX, USA).

3 Results

Instilled pleural liquid volume was 502 ± 158 mL. Normally aerated, collapsed and hyperinflated lung regions as computed by CT analysis, tidal mechanics expressed as compliances of respiratory system, lung and chest wall, and CT aeration regions of tidal recruiment and tidal hyperinflation during all experimental conditions are expressed in Table 1. The effect of the different experimental condition on respiratory P–V curve are shown in online supplementary (S2). The different SI values computed from Paw to Ptp traces in each steps of the study are represented in Fig. 1.

At baseline conditions, with PEEP 1 cmH_2O, SI (mean ± SD) computed from Paw was 0.6 ± 0.12 and mean CT-determined tidal recruitment was 18.8 ± 1.1 % of the tidal volume. In this "baseline" condition, the transpulmonary pressure SI (1.03 ± 0.22) seems to be unable to describe this effect. Indeed, with PEEP level set at 10 cmH_2O, SI increase with a concomitant reduction of tidal recruitment as determined by CT (8.9 ± 0.8 %) along with a minor increase of tidal hyperinflation (1.7 ± 0.4 %). The increased PEEP level in this baseline condition substantially reduced non-aerated and poorly aerated volumes, as confirmed by the reduction in TR and the increment in Cl (although not significant). After the instillation of pleural liquid (PE P1), even with an increase in CT tidal recruitment (26.1 ± 8.2 %), SIptp indicate a preponderant over-distension effect. Yet, the extent of tidal hyperinflation, never exceeded 1.3 %. After the increment in PEEP level (PE P10), the amount of CT-determined tidal recruitment decreased to 4.7 %, suggesting a huge recruitment effect of PEEP, as also reflected by the increment in lung compliance ($p < 0.05$). The SI in this case was substantially unaffected. The comparison between SI computed from Ptp with the corresponding values computed from Paw and a schematic view of the results compared with the CT images are shown in Fig. 2. Supplementary figures in the online resource show the results of Bland–Altman analysis of the relationship between SIpaw and SIptp and the individual animal relationship between SIpaw and SIptp with TR and TH.

4 Discussion

The major findings of this study are that with a normal respiratory system, the SI correctly suggested tidal recruitment at low level of PEEP, as documented by quantitative CT. However, in the same condition after the increment in PEEP level, SI, even when computed from Ptp, proved a misleading indicator of underlying lung distension and obscured tidal recruitment. With a unilateral pleural effusion model, extensive tidal recruitment can occur without significant overinflation, even though the SI values computed either from Paw to Ptp indicated otherwise.

The SI has been validated by clinical trials in ARDS patients without chest wall abnormalities and prior

Table 1 Comparisons among tested conditions regarding volume at end-expiration in normally aerated, poorly aerated, non-aerated and hyperinflated areas, compliances of respiratory system, lung and chest wall, and percentage of tidal recruitment/hyperinflation computed by CT scan

Conditions	Normally aerated (mL)	Non-aerated (mL)	Hyperinflated (mL)	Poorly areated (mL)	Crs (mL/cmH$_2$O)	Ccw (mL/cmH$_2$O)	Cl (mL/cmH$_2$O)	TR (%)	TH (%)
BSL P1	115.4 ± 27.6^{b,c,d}	13.0 ± 5.0^{b,c,d}	0.5 [0.3; 0.8]^{b}	68.5 ± 12.1^{b,c,d}	24.3 ± 2.8^{b,c}	72.2 ± 2.3^{b,c,d}	38.8 ± 3.1^{c}	18.8 ± 1.1^{b,c,d}	0.7 ± 0.2^{b,c,d}
BSL P10	239.0 ± 69.3^{a,c,d}	3.9 ± 1.3^{a,c}	1.0 [0.6; 3.7]^{a,c}	22.2 ± 6.6^{a,c,d}	34.8 ± 3.0^{a,c}	110 ± 1.5^{a}	42.8 ± 4.2^{c}	8.9 ± 0.8^{a,c,d}	1.7 ± 0.4^{a,c}
PE P1	39.8 ± 32.1^{a,b,d}	39.1 ± 18.1^{a,b,d}	0.3 [0.1; 0.4]^{b}	49.0 ± 26.4^{a,b,d}	18.1 ± 3.1^{a,b,d}	99.2 ± 1.5^{a}	25.5 ± 2.9^{a,b,d}	26.09 ± 8.2^{a,b,d}	1.3 ± 0.4^{a,d}
PE P10	210.3 ± 22.4^{a,b,c}	6.5 ± 2.7^{a,c}	0.7 [0.4; 2.0]	38.4 ± 5.7^{a,b,c}	31.2 ± 2.7^{a,c}	113.2 ± 2.8^{a}	44.6 ± 4.0^{c}	4.7 ± 1.3^{a,b,c}	3.3 ± 1.1^{a,b,c}

The table describe the CT distribution of lung volume, the modification of compliances and tidal recritment/hyperinfletion for each experimental conditions

BSL P1 baseline PEEP 1 cmH$_2$O, *BSL P10* baseline PEEP 10 cmH$_2$O, *PE P1* pleural effusion PEEP 1 cmH$_2$O, *PE P10* pleural effusion PEEP 10 cmH$_2$O, *Crs* respiratory system compliance, *CL* lung compliance, *Ccw* chest wall compliance, *Crs* respiratory system compliance, *TR* tidal recruitment *%*, *TH* tidal hyperinflation *%*

* $P < 0.001$

[a] $p < 0.05$ vs. BSL P1

[b] $p < 0.05$ vs. BSL P10

[c] $p < 0.05$ vs. PE P1

[d] $p < 0.05$ vs PE P10

experimental work has been confined to small animal lungs [8, 9, 28]. Terragni et al. [6] proposed the use of the dynamic airway opening *P/t* profile during constant flow to replace the static P/V curve. The same group previously described that a downward concavity on the *P/t* profile corresponded to a static P/V with a LIP and a continuous increment in compliance, while an upward concavity on the *P/t* profile corresponded to a static P/V curve with a distinct UIP and a continuous reduction in compliance [29]. Those analyses are based on the assumption that the rate of change of Paw is related to the change in lung compliance [30]. The threshold limit was defined in experimental sudies [8, 19] comparing the SI values with pulmonary histological damage and concentration of pro-inflammatory cytokines. In a recent experimental study, Grasso et al. [27] compared SI values—after expressly setting the ventilator to achieve different SI values—with CT scan. Quantitative CT analysis demonstrated a nonhomogeneous distribution of pulmonary alterations of the lung [31] and provided a quantitative imaging standard for assessing tidal recruitment.

In our previous study [24], conducted in a heterogeneously compromised large animal model, the SI reported always exceeded 1.0, even when the lung was compressed and PEEP was negligible. We showed how the lung was recruited impressively as tidal airway pressures rose or PEEP was added, and yet how the SI increased still further from an already elevated baseline.

In the present study, we analyzed the end-expiration and end-inspiration CT scans corresponding to the inspiratory *P/t* plots that make up the SI equation. In contrast with previous works, we chose one type of ventilation at two levels of PEEP, looking at possible changes in SI induced by PEEP itself as well as by pleural effusion. In the baseline condition, tidal compliance increased when PEEP rose to 10 cmH$_2$O, supporting the notion that b < 1.0 was indicative of tidal recruiment in that condition [8]. Moreover, considering that in the supine position, due to gravitational forces, the abdominal content exerts a positive pressure on the abdominal surface of the diaphragm, the diaphragm is displaced upward and resting lung volume decreases. The passive tension developed across the diaphragm in this way is responsible in part for the increase in the apparent stiffness of the chest wall [32] and for the decrease in chest-wall compliance observed at low lung volume. The application of PEEP can reduce the upward displacement of the diaphragm-abdominal compartment into the thorax and move the chest wall into the more vertical linear portion of the classical P–V chest wall compliance curve, which in its lowest zone of volume near residual volume is convex to the x-axis. In our animal model, the effect of PEEP application in baseline supine conditions reduces tidal recruitment of the lung

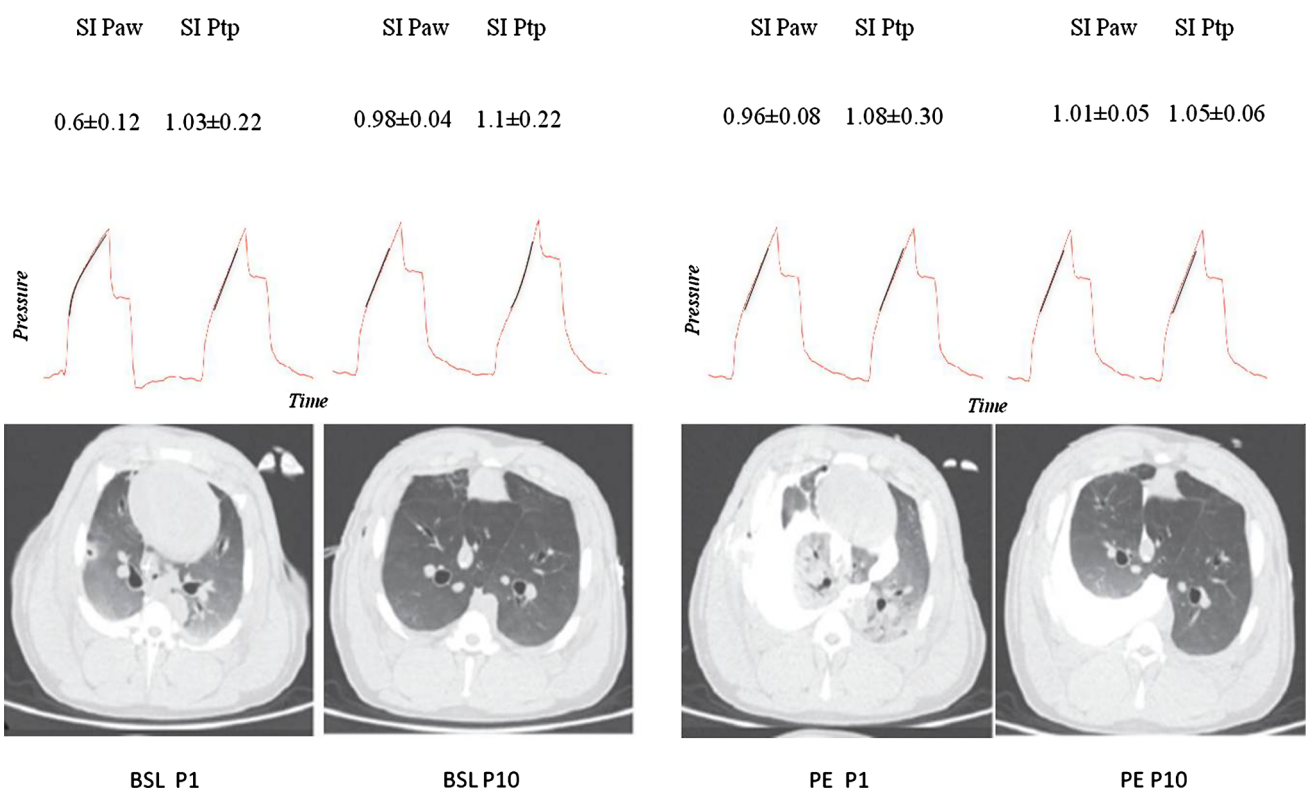

Fig. 2 The figure represent a schematic view of results expressed as Stress index computed from airway (Paw) and transpulmonary (Ptp) pressures, compared with computed tomography of the chest. *SI* Stress index, *BSL P1* baseline PEEP 1 cmH_2O, *BSL P10* baseline PEEP 10 cmH_2O, *PE P1* pleural effusion PEEP 1 cmH_2O, *PE P10* pleural effusion PEEP 10 cmH_2O

parenchyma and at the same time, increments chest wall compliance, as expected. The contribution of PEEP in lifting and tilting the heart off the esophagus should also be considered, but this effect is likely to have been quite small in magnitude [33, 34]. We acknowledge that a study on healthy subjects [35] showed how chest wall compliance is not modified by application of PEEP. Indeed, inter-species factors may explain, at least in part, this difference. Moreover, in another study by the same group, performed in anesthetized patients undergoing mechanical ventilation for acute ventilatory failure [36], chest wall compliance did actually improve with PEEP application. Again, many factors may explain such a differing behaviour, such as a different degree of abdominal distension or the administration of narcotic sedation or the presence of tissue oedema.

As for the effects of the effusion on the respiratory system, pleural effusion indeed modified its mechanics, reducing Crs and Cl and incrementing Ccw, along with a marked reduction in normally aerated volume and a significant increment in non-aerated and poorly-aerated volumes. Moreover, the increment in PEEP in the presence of pleural effusion restored the normally aerated volume, reducing significantly both non/poorly aerated areas. The same effect was detected by CT with a significant reduction in TR between PEEP 1 and PEEP10. Because the chest wall operates in series with the mechanically interdependent lung compartment, abnormalities affecting either structure (such as pleural effusion) can be partially accommodated by deformation of its counterpart. Lung inflation displace effusion towards the flexible regions of the chest wall (normally those bordered by the diaphragm). Lung expansion at the side of moderate effusion was shown not to differ from that at the other side, suggesting that the ipsilateral lung might be displaced as well as compressed by the effusion. The accumulation of effusion disrupts the reciprocal lung–chest wall conformation: the chest wall expands outwards while the adjacent lung is compressed, decoupling the properties of the lung and chest wall. The normal aeration volume dramatically decreased after pleural effusion instillation (from 115.4 to 39.8 mL, in average), and the increment of PEEP restored the aerated volume to baseline values, incrementing all the compliances.

Although tidal recruitment coexisted with very little hyperinflation, SI only suggested a preponderance of overdistension at both PEEP levels, and the reduction of recruitment with the increments of PEEP was not reflected by change in SI, even when Ptp was used. With pleural effusion, low-pressure tidal recruitment could take place as

a compliant chest wall that cyclically relieves the space occupying effect and hydrostatic lung compression accepts the fluid.

The difference between ΔPaw and ΔPes is generally considered a valid estimate of ΔPtp [37]. However, absolute values of Pes can be influenced by asymmetry of lung disease, lung and chest wall distortion, increased abdominal pressure, large pleural effusions and by calibration of the cathether [13, 37, 38]. As consequence, a debate exists as to whether Pes remains an acceptable estimator of average Ppl [39]. The lack of ability of SI as calculated from Ptp/*t* curve to detect the mechanical qualities of the lung is a likely consequence of the inability of absolute values of Pes to reflect absolute values of average Ppl [40]. In fact, the assumption that Pes accurately represents average Ppl is higly controversial, due to the roles of elastance of the esophageal catheter, tone of the esophageal wall, weight of the mediastinic organs and patient position, all of which could alter the measured value so that the absolute esophageal pressure would not reflect Ppl [33, 38, 41, 42]. Furthermore, in an experimental model Pes was found to be quite similar to the pressure of the pleural space measured in the middle part of the lung, while it overestimated and underestimated Ppl in the non-dependent and dependent lung regions, respectively [43]. In contrast, variations in Ppl are similar to those in Pes at each lung level [41, 44, 45]. In the present study, after having artificially altered the lung and chest wall compliances, we confirmed that the ability of SI to predict tidal recruitment and overdistension was significantly reduced, even if the index was computed from the Ptp profile. Indeed, the SI did not vary across experimental conditions, despite markedly different amounts of underlying tidal recruitment.

4.1 Study limitations

As a laboratory-based experimental study conducted in supine normal animals, our results are relevant to this model but cannot be translated without reservation to the clinical setting. Although similar to the human, the thorax, abdomen and mediastinum of the pig differ somewhat. Among patients, the influence of pleural liquid on the chest wall is likely to vary with its conformation and baseline compliance. The associated impact on the computed SI cannot be easily predicted. Thus, the magnitude of the effects we describe here will likely vary with the volume of instilled pleural liquid, even if we choose only one volume of effusion based on our previous observation. The protocols steps were not randomized, and each step was at least 3 h long. Indeed, we cannot exclude that our results are due, at least in part, to some carry-over effect. Finally, in our model the lung and the chest wall were intrinsically normal, and the observed deformations of the lung and chest wall were the result of their relative adaptations to pleural fluid accumulation and airway pressure. Stiffening of the chest wall or limitations of lung compressibility–as often occur in the clinical setting—should therefore modify the magnitude (but not the direction) of the responses we reported.

5 Conclusions

In a unilateral pleural effusion experimental model with different levels of PEEP, our results suggest that SI can be ambiguous under multi-compartmental conditions of heterogeneous collapse and extensive recruitment, even if calculated from a Ptp tracing. An interpretation of the SI in conjunction with tidal compliances could help better identify the actual underlying behaviors.

Author's contribution F.P., G.F., A.A. and M.J.: Study design; F.P., G.J., A.A. and D.D.: Animal preparation, data collection; F.P. and M.U: Data analysis and drafting the first version of the paper; M.J, P.F., M.U.: revision of the paper.

Funding This work was supported by departmental funding only.

Compliance with ethical standards

Conflict of interest The authors state that they have no conflict of interest to declare.

References

1. Hickling KG. The pressure-volume curve is greatly modified by recruitment. A mathematical model of ARDS lungs. Am J Respir Crit Care Med. 1998;158(1):194–202. doi:10.1164/ajrccm.158.1.9708049.
2. Jonson B, Richard JC, Straus C, Mancebo J, Lemaire F, Brochard L. Pressure-volume curves and compliance in acute lung injury: evidence of recruitment above the lower inflection point. Am J Respir Crit Care Med. 1999;159(4 Pt 1):1172–8. doi:10.1164/ajrccm.159.4.9801088.
3. Suter PM, Fairley B, Isenberg MD. Optimum end-expiratory airway pressure in patients with acute pulmonary failure. New Engl J Med. 1975;292(6):284–9. doi:10.1056/NEJM197502062920604.
4. Matamis D, Lemaire F, Harf A, Brun-Buisson C, Ansquer JC, Atlan G. Total respiratory pressure-volume curves in the adult respiratory distress syndrome. Chest. 1984;86(1):58–66.
5. Amato MB, Barbas CS, Medeiros DM, Magaldi RB, Schettino GP, Lorenzi-Filho G, Kairalla RA, Deheinzelin D, Munoz C, Oliveira R, Takagaki TY, Carvalho CR. Effect of a protective-ventilation strategy on mortality in the acute respiratory distress syndrome. New Engl J Med. 1998;338(6):347–54. doi:10.1056/NEJM199802053380602.
6. Terragni PP, Rosboch GL, Lisi A, Viale AG, Ranieri VM. How respiratory system mechanics may help in minimising ventilator-

induced lung injury in ARDS patients. Eur Respir J Suppl. 2003;42:15s–21s.
7. Hess DR. Respiratory mechanics in mechanically ventilated patients. Respir Care. 2014;59(11):1773–94. doi:10.4187/respcare.03410.
8. Ranieri VM, Zhang H, Mascia L, Aubin M, Lin CY, Mullen JB, Grasso S, Binnie M, Volgyesi GA, Eng P, Slutsky AS. Pressure-time curve predicts minimally injurious ventilatory strategy in an isolated rat lung model. Anesthesiology. 2000;93(5):1320–8.
9. Terragni PP, Filippini C, Slutsky AS, Birocco A, Tenaglia T, Grasso S, Stripoli T, Pasero D, Urbino R, Fanelli V, Faggiano C, Mascia L, Ranieri VM. Accuracy of plateau pressure and stress index to identify injurious ventilation in patients with acute respiratory distress syndrome. Anesthesiology. 2013;119(4):880–9. doi:10.1097/ALN.0b013e3182a05bb8.
10. Graf J. Pleural effusion in the mechanically ventilated patient. Curr Opin Crit Care. 2009;15(1):10–7. doi:10.1097/MCC.0b013e3283220e4a.
11. Formenti P, Umbrello M, Piva IR, Mistraletti G, Zaniboni M, Spanu P, Noto A, Marini JJ, Iapichino G. Drainage of pleural effusion in mechanically ventilated patients: time to measure chest wall compliance? J Crit Care. 2014;29(5):808–13. doi:10.1016/j.jcrc.2014.04.009.
12. Formenti P, Umbrello M. Pleural effusion in ARDS. Minerva Anestesiol. 2014;80(2):245–53.
13. Krell WS, Rodarte JR. Effects of acute pleural effusion on respiratory system mechanics in dogs. J Appl Physiol. 1985;59(5):1458–63.
14. Sousa AS, Moll RJ, Pontes CF, Saldiva PH, Zin WA. Mechanical and morphometrical changes in progressive bilateral pneumothorax and pleural effusion in normal rats. Euro Respir J. 1995;8(1):99–104.
15. Graf J, Formenti P, Santos A, Gard K, Adams A, Tashjian J, Dries D, Marini JJ. Pleural effusion complicates monitoring of respiratory mechanics. Crit Care Med. 2011;39(10):2294–9. doi:10.1097/CCM.0b013e3182227bb5.
16. Plataki M, Hubmayr RD. Should mechanical ventilation be guided by esophageal pressure measurements? Curr Opin Crit Care. 2011;17(3):275–80. doi:10.1097/MCC.0b013e328344dda6.
17. Talmor D, Sarge T, Malhotra A, O'Donnell CR, Ritz R, Lisbon A, Novack V, Loring SH. Mechanical ventilation guided by esophageal pressure in acute lung injury. New Engl J Med. 2008;359(20):2095–104. doi:10.1056/NEJMoa0708638.
18. Staffieri F, Stripoli T, De Monte V, Crovace A, Sacchi M, De Michele M, Trerotoli P, Terragni P, Ranieri VM, Grasso S. Physiological effects of an open lung ventilatory strategy titrated on elastance-derived end-inspiratory transpulmonary pressure: study in a pig model*. Crit Care Med. 2012;40(7):2124–31. doi:10.1097/CCM.0b013e31824e1b65.
19. Chiumello D, Gattinoni L. Stress index in presence of pleural effusion: Does it have any meaning? Intensive Care Med. 2011;37(4):561–3. doi:10.1007/s00134-011-2134-3.
20. Higgs BD, Behrakis PK, Bevan DR, Milic-Emili J. Measurement of pleural pressure with esophageal balloon in anesthetized humans. Anesthesiology. 1983;59(4):340–3.
21. Dechman G, Sato J. Bates JH (1992) Factors affecting the accuracy of esophageal balloon measurement of pleural pressure in dogs. J Appl Physiol. 1985;72(1):383–8.
22. Chiumello D, Consonni D, Coppola S, Froio S, Crimella F, Colombo A. The occlusion tests and end-expiratory esophageal pressure: measurements and comparison in controlled and assisted ventilation. Annal Intensive Care. 2016;6(1):13. doi:10.1186/s13613-016-0112-1.
23. Huggins JT, Doelken P, Sahn SA, King L, Judson MA. Pleural effusions in a series of 181 outpatients with sarcoidosis. Chest. 2006;129(6):1599–604. doi:10.1378/chest.129.6.1599.
24. Formenti P, Graf J, Santos A, Gard KE, Faltesek K, Adams AB, Dries DJ, Marini JJ. Non-pulmonary factors strongly influence the stress index. Intensive Care Med. 2011;37(4):594–600. doi:10.1007/s00134-011-2133-4.
25. Chiumello D, Marino A, Brioni M, Menga F, Cigada I, Lazzerini M, Andrisani MC, Biondetti P, Cesana B, Gattinoni L. Visual anatomical lung CT scan assessment of lung recruitability. Intensive Care Med. 2013;39(1):66–73. doi:10.1007/s00134-012-2707-9.
26. Graf J, Mentzelopoulos SD, Adams AB, Zhang J, Tashjian JH, Marini JJ. Semi-quantitative tracking of intra-airway fluids by computed tomography. Clin Physiol Funct Imaging. 2009;29(6):406–13. doi:10.1111/j.1475-097X.2009.00885.x.
27. Grasso S, Terragni P, Mascia L, Fanelli V, Quintel M, Herrmann P, Hedenstierna G, Slutsky AS, Ranieri VM. Airway pressure-time curve profile (stress index) detects tidal recruitment/hyperinflation in experimental acute lung injury. Crit Care Med. 2004;32(4):1018–27.
28. de Perrot M, Imai Y, Volgyesi GA, Waddell TK, Liu M, Mullen JB, McRae K, Zhang H, Slutsky AS, Ranieri VM, Keshavjee S. Effect of ventilator-induced lung injury on the development of reperfusion injury in a rat lung transplant model. J Thorac cardiovasc surg. 2002;124(6):1137–44. doi:10.1067/mtc.2002.125056.
29. Ranieri VM, Giuliani R, Fiore T, Dambrosio M, Milic-Emili J. Volume-pressure curve of the respiratory system predicts effects of PEEP in ARDS: "occlusion" versus "constant flow" technique. Am J Respir Crit Care Med. 1994;149(1):19–27. doi:10.1164/ajrccm/149.2_Pt_2.S19.
30. D'Angelo E, Prandi E, Tavola M, Robatto FM. Assessment of respiratory system viscoelasticity in spontaneously breathing rabbits. Respir Physiol. 1998;114(3):257–67.
31. Gattinoni L, Caironi P, Pelosi P, Goodman LR. What has computed tomography taught us about the acute respiratory distress syndrome? Am J Respir Crit Care Med. 2001;164(9):1701–11. doi:10.1164/ajrccm.164.9.2103121.
32. Mutoh T, Lamm WJ, Embree LJ, Hildebrandt J, Albert RK. Albert RKAbdominal distension alters regional pleural pressures and chest wall mechanics in pigs in vivo. J Appl Physiol. 1991;70(6):2611–8.
33. Marini JJ, O'Quin R, Culver BH, Butler J. Estimation of transmural cardiac pressures during ventilation with PEEP. J Appl Physiol Respir Environ Exerc Physiol. 1982;53(2):384–91.
34. O'Quin RJ, Marini JJ, Culver BH. Butler J (1985) Transmission of airway pressure to pleural space during lung edema and chest wall restriction. J Appl Physiol. 1985;59(4):1171–7.
35. Pelosi P, Ravagnan I, Giurati G, Panigada M, Bottino N, Tredici S, Eccher G, Gattinoni L. Positive end-expiratory pressure improves respiratory function in obese but not in normal subjects during anesthesia and paralysis. Anesthesiology. 1999;91(5):1221–31.
36. Musch G, Foti G, Cereda M, Pelosi P, Poppi D, Pesenti A. Lung and chest wall mechanics in normal anaesthetized subjects and in patients with COPD at different PEEP levels. Euro Respir J. 1997;10(11):2545–52.
37. Akoumianaki E, Maggiore SM, Valenza F, Bellani G, Jubran A, Loring SH, Pelosi P, Talmor D, Grasso S, Chiumello D, Guerin C, Patroniti N, Ranieri VM, Gattinoni L, Nava S, Terragni PP, Pesenti A, Tobin M, Mancebo J, Brochard L. The application of esophageal pressure measurement in patients with respiratory failure. Am J Respir Crit Care Med. 2014;189(5):520–31. doi:10.1164/rccm.201312-2193CI.
38. Mojoli F, Iotti GA, Torriglia F, Pozzi M, Volta CA, Bianzina S, Braschi A, Brochard L. In vivo calibration of esophageal pressure in the mechanically ventilated patient makes measurements reliable. Crit Care. 2016;20(1):98. doi:10.1186/s13054-016-1278-5.

39. Pecchiari M, Loring SH, D'Angelo E. Esophageal pressure as an estimate of average pleural pressure with lung or chest distortion in rats. Respir Physiol Neurobiol. 2013;186(2):229–35. doi:10.1016/j.resp.2013.02.006.
40. Brander L, Ranieri VM, Slutsky AS. Esophageal and transpulmonary pressure help optimize mechanical ventilation in patients with acute lung injury. Crit Care Med. 2006;34(5):1556–8. doi:10.1097/01.CCM.0000216146.51250.8D.
41. Milic-Emili J, Mead J, Turner JM, Glauser EM. Improved technique for estimating pleural pressure from esophageal balloons. J Appl Physiol. 1964;19:207–11.
42. Hedenstierna G. Airway closure: nothing good during anesthesia. Minerva Anestesiol. 2012;78(11):1193–5.
43. Pelosi P, Goldner M, McKibben A, Adams A, Eccher G, Caironi P, Losappio S, Gattinoni L, Marini JJ. Recruitment and derecruitment during acute respiratory failure: an experimental study. Am J Respir Crit Care Med. 2001;164(1):122–30. doi:10.1164/ajrccm.164.1.2007010.
44. Gillespie DJ, Lai YL, Hyatt RE. Comparison of esophageal and pleural pressures in the anesthetized dog. J Appl Physiol. 1973;35(5):709–13.
45. Chiumello D, Cressoni M, Colombo A, Babini G, Brioni M, Crimella F, Lundin S, Stenqvist O, Gattinoni L. The assessment of transpulmonary pressure in mechanically ventilated ARDS patients. Intensive Care Med. 2014;40(11):1670–8. doi:10.1007/s00134-014-3415-4.